

## Fission fragment angular distributions: A probe to study heavy-ion fusion dynamics

R. G. Thomas,<sup>1</sup> R. K. Choudhury,<sup>1,2</sup> A. K. Mohanty,<sup>1</sup> A. Saxena,<sup>1</sup> and S. S. Kapoor<sup>1</sup>

<sup>1</sup>*Bhabha Atomic Research Centre, Mumbai 400 085, India*

<sup>2</sup>*Institute of Physics, Bhubaneswar 751005, India*

(Received 13 August 2002; revised manuscript received 19 December 2002; published 7 April 2003)

It is shown that when fusion is initiated at relatively larger distances due to the presence of rotational couplings, the Businaro-Gallone barrier shifts towards higher mass asymmetry, thus favoring further mass equilibration towards symmetric configurations. This leads to the occurrence of preequilibrium fission events for all systems which affect the fission fragment angular distributions at subbarrier energies. The fission fragment angular distributions calculated as an admixture of compound nuclear and preequilibrium components explains quite well the energy dependence of the angular anisotropies for many systems around the actinide regions irrespective of the entrance channel mass asymmetries at energies both well below and above the Coulomb barrier. From the fits to the angular distributions,  $K$ -equilibration time is deduced to be  $\sim 6 \times 10^{-20}$  s for a temperature  $\sim 1$  MeV.

DOI: 10.1103/PhysRevC.67.041601

PACS number(s): 25.70.Jj, 24.75.+i

It is noticed in several cases of heavy-ion-induced fission reactions involving actinide target nuclei that the fragment anisotropies are significantly larger than the statistical saddle point model (SSPM) predictions [1,2], and this anomalous behavior of the fragment anisotropies has been a subject of extensive investigations both experimentally and theoretically [3–10] in recent years. It has been pointed out earlier [4] that anomalous fragment anisotropies can arise due to an admixture of compound-nucleus fission (CNF) and noncompound nucleus fission (NCNF) events in case of highly fissile target nuclei. There is also currently much interest in determining the optimum entrance channel conditions to maximize the probability of compound nucleus formation leading to heavy and superheavy nuclei without loss of flux to non-equilibrium fissionlike processes [11,12]. Thus, the study of fragment anisotropies can serve as a useful probe to determine the admixture of the noncompound fissionlike processes, in heavy-ion-induced fission reactions, which in turn can guide in selecting optimum entrance channel conditions for the synthesis of superheavy nuclei.

Two processes of NCNF events, namely, quasifission (QF) and fast fission are known to occur in heavy-ion-induced reactions under certain conditions. Theoretically, quasifission is predicted when the product  $Z_1 Z_2$  of the atomic numbers of target and projectile exceeds around 1600, and fast fission is expected to be significant only for very large values of the compound nucleus ( $Z^2/A$ ) and angular momentum  $J$  when the fission barrier becomes vanishingly small. In the case of heavy-ion reactions induced by light projectiles such as B, C, O, and F on the actinide targets, where none of these conditions are satisfied, the observed anomalous anisotropies for these cases have been understood on the basis of a different NCNF mechanism, termed as preequilibrium fission (PEF) [4].

The mechanism of PEF can be visualized as follows. After reaching the contact configuration, along the entrance channel trajectory, the composite system relaxes in various degrees of freedom governed principally by the multidimensional potential energy landscape. The relaxation in mass-asymmetry degree is known to depend on the entrance chan-

nel mass asymmetry,  $\alpha$  ( $= (A_T - A_P)/(A_T + A_P)$ ) with respect to the Businaro-Gallone critical value  $\alpha_{BG}$ . If  $\alpha > \alpha_{BG}$ , there is a driving force to increase mass asymmetry in the subsequent dynamics, favoring amalgamation of the two interacting nuclei, to form a compound nucleus that mostly undergoes fission in case of actinide target nuclei. On the other hand, for  $\alpha < \alpha_{BG}$ , the projectile-target system relaxes towards a symmetric dinuclear system. For the light projectile-heavy target systems studied in this work, the unconditional fission saddle is more elongated than the contact configuration of the entrance channel where the system is initially trapped towards fusion. For such cases, the system moves towards the path of compound-nucleus formation in the subsequent dynamics involving transition from the sudden potential to the adiabatic one. Considering that the equilibration in the elongation degree of freedom is much slower than in the mass-asymmetry degree of freedom, the dynamical trajectories are expected to get injected into the fission valley at different points between the compound nucleus and the saddle point configurations corresponding to the different initial radial separation  $\rho$  at the contact point of fusion. Here  $\rho = r/(R_1 + R_2)$ , where  $r$  is the center-to-center separation and  $R_1$  and  $R_2$  are the radii of the two spherical nuclei. Subsequently, there is, in general, a large probability for the intermediate system to roll down the potential energy curve towards the mononuclear configuration, leading to the formation of a compound nucleus that mostly decays by fission in the case of heavy systems. However, there can also be a significant probability for the intermediate excited dinuclear system to undergo reseparation/fission (preequilibrium fission) while on its way to the formation of a compound nucleus. The probability of preequilibrium fission will be governed by an effective barrier height against fission, which is experienced by the intermediate system on entry into the fission valley. This effective barrier height  $\delta$  would correspond to the height of the unconditional saddle as measured with respect to the potential energy of the intermediate system configuration, and can be written as  $\delta = x B_f$ . Here,  $B_f$  is the normal fission barrier height that is measured with respect to the potential energy of the compound-nucleus con-

figuration, and  $x$  is a physical parameter whose value depends on the point at which the intermediate system configuration meets the fission valley, and thereby on the value of  $\rho$  involved at the contact point of fusion. Since the potential energy of an elongated intermediate system is larger than that of the compound nucleus,  $x$  should be less than 1. Clearly, in this picture  $x=1$  will correspond to compound-nucleus fission, and  $x=0$  will correspond to the case (quasifission) where  $\rho$  is sufficiently large such that injection into the fission valley is beyond the saddle point deformation, and the system does not experience any barrier along the path of reseparation. Therefore a gradual transition from QF to PEF to CNF is expected as  $\rho$  decreases. Measurements of the fragment anisotropies can help us to identify the contributions from these different processes.

The  $K$  distributions of PEF will be the product of the entrance channel  $K$  distribution and the saddle point  $K$  distribution [5,6,8], and the narrower of the above two  $K$  distributions governs the fragment anisotropy. This explains the observed larger anisotropies whenever the input  $K$  distribution is not fully equilibrated. Thus, the PEF mechanism can lead to anomalous fission fragment anisotropies, if the system relaxes towards mass-symmetric dinuclear shape as is the case for  $\alpha < \alpha_{BG}$ . For  $\alpha > \alpha_{BG}$ , the intermediate system moves towards a mononuclear shape, and therefore the observed anisotropies should be in agreement with the SSPM. In case of bombarding energies above fusion barrier, this prediction has been experimentally verified [1]. However, there have been apparent deviations from the above picture in the sub-barrier fusion reactions in the cases of  $^{10,11}\text{B}, ^{12}\text{C}$  induced reactions on actinide targets (corresponding to  $\alpha > \alpha_{BG}$ ). While the observed anisotropies are consistent with the SSPM for above barrier energies, the anisotropies for sub-barrier fusion are found to be anomalously large. An important aspect which has not been considered so far is the effect of channel couplings on the subsequent fission dynamics after being captured from the entrance channel, although it has been included in to estimate the fusion probability correctly. In this work, it is shown that with the inclusion of channel coupling effects, the observed heavy-ion fission fragment anisotropies both below and above Coulomb barrier energies can be explained by considering fission events as an admixture of CNF and PEF components. In what follows, we show that due to a shifted BG point at sub-barrier energies, the PEF model can explain fragment anisotropy data for all projectile-target combinations, both below and above barrier energies.

The Businaro-Gallone critical mass asymmetry  $\alpha_{BG}$  is determined by maximizing the potential energy with respect to  $\alpha$ , allowing all shape degrees of freedom to vary. However, on the assumption that the relaxation in the separation coordinate is much slower than in mass-asymmetry degree of freedom, one would expect that mass flow in the early stages of equilibration following neck formation of the dinuclear complex will be governed by the potential energies corresponding to the given value of internuclear separation  $\rho$  at fusion. It may be noted that the value of  $\rho$  at fusion varies significantly as a function of the bombarding energy across the fusion barrier. We have calculated the potential energies

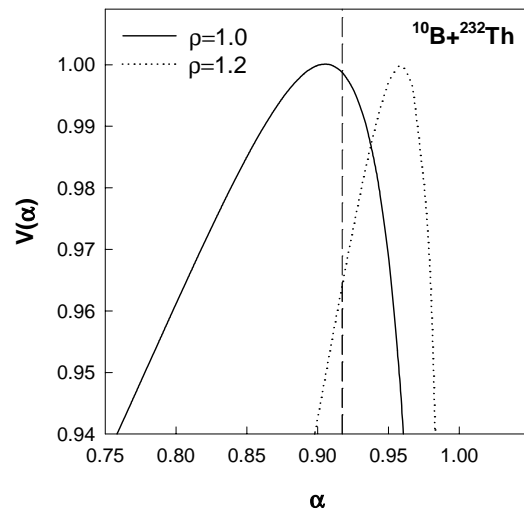


FIG. 1. The potential energy,  $V(\alpha, \rho)$  (in arbitrary unit) with respect to sphere as a function of  $\alpha$  for different values of  $\rho$ . The peak values are normalized to unity. The vertical dashed line gives the  $\alpha$  value of the entrance channel.

for different values of  $\rho$  using the shape parametrization of Swiatecki, which consists of two spheres connected by a conical neck [13,14]. Figure 1 shows the plot of the potential energy  $V(\alpha)$  (with respect to sphere) as a function of  $\alpha$  for the  $^{10}\text{B} + ^{232}\text{Th}$  compound system for  $\rho=1$  and 1.2. The vertical dashed line in the figure shows the mass asymmetry of the entrance channel. This result shows that  $^{10}\text{B} + ^{232}\text{Th}$  system, which corresponds to the right side of the peak (or  $\alpha > \alpha_{BG}$ ) for  $\rho=1$ , turns out to be on the left side of the BG peak (or  $\alpha < \alpha_{BG}$ ) for  $\rho=1.2$ . Thus even for the systems with  $\alpha > \alpha_{BG}$ , if fusion is initiated at a larger distance, as in the case of collisions with the tips of the deformed nuclei at sub-barrier energies, the mass equilibration in the early stages favors evolution of the system towards a mass-symmetric shape before equilibration is achieved in the  $\rho$  degree of freedom. Consequently, in the sub-barrier fusion reactions of B+Th or C+Th, the potential energy drives the dynamical trajectories towards the symmetric fission valley. But in the above barrier fusion, these systems behave like  $\alpha > \alpha_{BG}$  to proceed to a mononuclear configuration before fission. One can thus understand the origin of the anomalous fragment anisotropies observed in the sub-barrier fusion even for the target-projectile combinations with  $\alpha > \alpha_{BG}$ .

We describe below the theoretical formalism to calculate fragment anisotropies taking into account the PEF component. We propose here that for  $T_\beta \leq T_0$  (where  $T_\beta$  and  $T_0$  are the transmissions through the eigenchannel  $\beta$ , corresponding to the barrier  $V_\beta$  and the uncoupled barrier  $V_0$ , respectively), the collision trajectory will lead to a compact configuration for which  $\rho \leq \rho_0$  (where  $\rho_0$  is the internuclear separation of two spherical nuclei at the contact point). On the other hand, for  $T_\beta > T_0$ , we assume that the dinuclear configuration will have  $\rho > \rho_0$ . After being captured into the conditional trajectory, the system will relax in mass degree of freedom and will meet the unconditional trajectory at different points. Therefore, the effective barrier height  $\delta$  and also the resulting escape probability  $f$  of PEF will depend on the entry

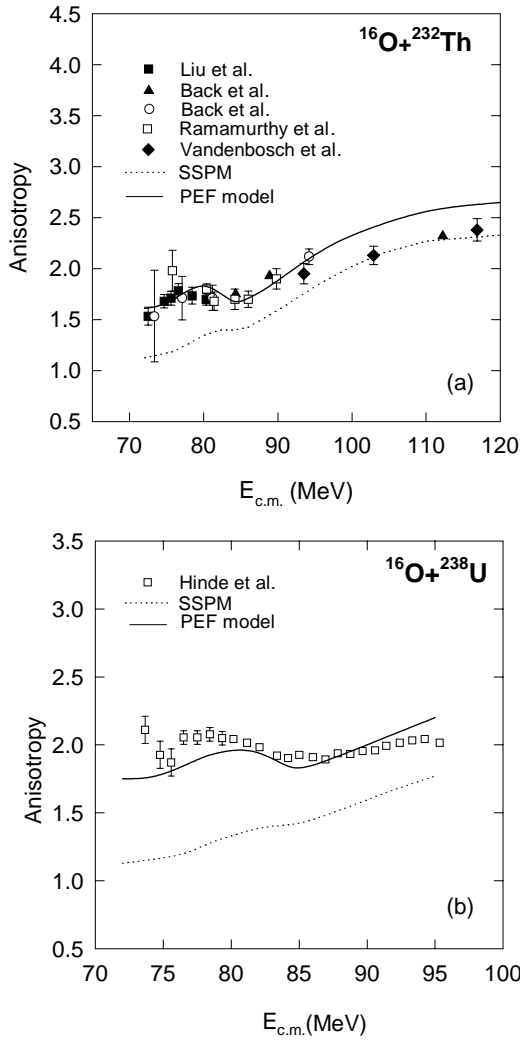


FIG. 2. Calculated fission fragment anisotropies on the basis of SSPM and PEF models along with experimental results for  $^{16}\text{O} + ^{232}\text{Th}$  [1,3,19,20] and  $^{16}\text{O} + ^{238}\text{U}$  [21] systems corresponding to  $\alpha < \alpha_{BG}$ .

point to the unconditional saddle point curve. In an actual dynamical trajectory calculation, one expects the effective barrier height  $\delta$  to continuously vary with the value of  $\rho$ , which in turn depends on the angle between the internuclear axis and the target deformation axis at the contact point. As mentioned earlier, we take into account this feature by involving a barrier scaling parameter  $x$  under the simplifying assumption that for  $\rho > \rho_0$ , the average effective fission barrier height is reduced by a factor  $x$ , while for  $\rho \leq \rho_0$ , full fission barrier height  $B_f$  is encountered. The mean fission time  $t_f$  is then given by

$$t_f(J) = \frac{2\pi}{\omega_{eq}} \exp\left(\frac{x B_f(J)}{\tau}\right) \quad \text{for } T_\beta(J) > T_0(J),$$

$$t_f(J) = \frac{2\pi}{\omega_{eq}} \exp\left(\frac{B_f(J)}{\tau}\right) \quad \text{for } T_\beta(J) \leq T_0(J), \quad (1)$$

where  $B_f(J)$  is the fission barrier,  $\tau$  is the temperature, and  $\omega_{eq}$  is set to  $10^{21} \text{ s}^{-1}$ . All the quantities are calculated as a function of the angular momentum  $J$  of the collision. Now if the equilibration time in the  $K$  degree of freedom of the dinuclear complex is  $t_K$ , then the fraction  $f(J)$  which escapes by PEF before reaching equilibrium in the  $K$  degree of freedom is given by

$$f(J) = [1 - \exp\{-t_K/t_f(J)\}]. \quad (2)$$

The above expression for  $f(J)$  is valid for systems with  $\alpha < \alpha_{BG}$ . Even the cases of  $\alpha > \alpha_{BG}$  wherein fusion occurs via the eigenchannel  $\beta$  corresponding to  $T_\beta > T_0$ , the above expression holds good, since in these cases the dynamical evolution to compound nucleus goes via a symmetric dinuclear shape. However, for  $\alpha > \alpha_{BG}$  and  $\beta$  corresponding to  $T_\beta \leq T_0$ , preequilibrium fission is not possible and  $f(J) = 0$ .

The fission fragment yield  $W(\theta)$  at an angle  $\theta$  can be written as

$$W(\theta) = \sum_{\beta} P_{\beta} [W_1(\beta, \theta) + W_2(\beta, \theta)], \quad (3)$$

where  $P_{\beta}$  is the probability of fusion from the eigenchannel  $\beta$ . In the case of deformed nuclei, the probability  $P_{\beta}$  is replaced by  $\sin(\omega)$  and the summation is carried out over  $\omega$ , the orientation angle between the internuclear axis and the target deformation axis.

$W_1(\beta, \theta)$  and  $W_2(\beta, \theta)$  are the fragment angular distributions for the CNF and PEF, respectively, and are given by

$$W_1(\beta, \theta) = \pi \lambda^2 \sum_{J=0}^{J_{max}} \sum_M^M [1 - f(J)] \times (2J+1) T_J(\beta) \times \sum_{K=-J}^J \frac{(2J+1) |d_{M,K}^J(\theta)|^2 F_S(K)}{4\pi \sum_{K=-J}^J F_S(K)}, \quad (4)$$

$$W_2(\beta, \theta) = \pi \lambda^2 \sum_{J=0}^{J_{max}} \sum_M^M f(J) \times (2J+1) T_J(\beta) \times \sum_{K=-J}^J \frac{(2J+1) |d_{M,K}^J(\theta)|^2 F_P(K)}{4\pi \sum_{K=-J}^J F_P(K)}. \quad (5)$$

Here  $F_S(K)$  is the  $K$  distribution at the saddle point given by  $F_S(K) = \exp\{-K^2/2K_0^2\}$ , with  $K_0 = \sqrt{I_{eff}\tau/\hbar^2}$ ,  $I_{eff}$  the effective moment of inertia;  $F_P(K)$  is the  $K$ -distribution function for the PEF events, which can be written as the product of the initial  $K$  distribution  $F_I(K)$  [ $F_I(K) = \exp\{-K^2/2\sigma_K^2(J)\}$ ] and the saddle point distribution  $F_S(K)$ . It is to be noted that in the present model, the symmetry axis of the fissioning nucleus is not the same as the target deformation axis, and therefore the initial  $K$  distribution is not depen-

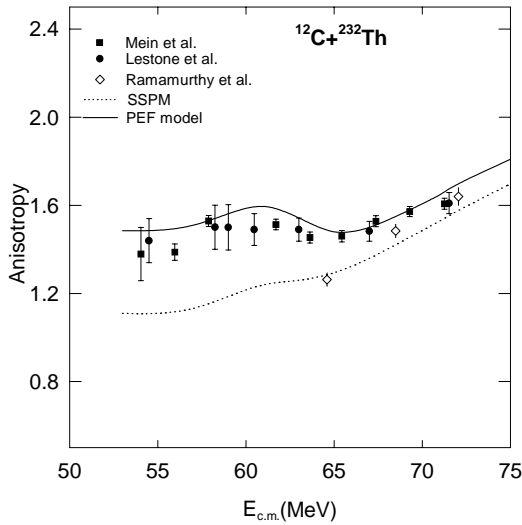


FIG. 3. Same as Fig. 2 for the  $^{12}\text{C}+^{232}\text{Th}$  [9] system ( $\alpha > \alpha_{BG}$ ).

dent on the angle  $\omega$  as assumed by Vorkapic and Ivanisevic [6] and Lestone *et al.* [8] in the entrance channel dependent  $K$ -state model. For the variance of the initial  $K$  distribution, we use  $\sigma_K(J) = q\sqrt{\tau t}J$ , where  $t$  is the fission time and  $q$  is the speed of  $K$  equilibration [8,15]. A fully equilibrated  $K$  distribution can be approximated as a flat (isotropic) distribution with all  $K$ 's equally populated. It can be seen that  $F_I(K)$  will approach a nearly flat distribution (say up to  $\sim 90\%$ ) for  $\sigma_K \sim 2J$ . Thus an estimate of the  $K$ -equilibration time  $t_K$  can be obtained from the relation  $t_K = 4/(q^2\tau)$ .

In order to make comparison with the experimental data, the fragment anisotropies were calculated at different energies for various systems, for various values of  $x$  and  $q$ . The deformation parameters  $\beta_2, \beta_4$  were taken as 0.22, 0.09 and 0.28, 0.05 for Th and U, respectively, for all the calculations. The saddle point effective moments of inertia and fission barriers were calculated using Sierk's model [16]. It was found that for  $x \approx 0.3$  and  $q \approx 8 \times 10^9 (\text{MeV s})^{-1/2}$ , the best  $\chi^2$  fits to the observed anisotropies are obtained for the various systems studied here. The fission fragment anisotropies calculated using Eq. (3) for systems involving actinide deformed target nuclei and zero target/projectile spins are shown in Figs. 2 and 3 with the above choice of  $x$  and  $q$ .

In case of nonzero target/projectile spins, the effect of target or projectile spin on angular distributions due to different  $M$ -state distributions is negligible for heavy-ion-induced reactions. However, its effect on  $K$  distribution cannot be ignored particularly at sub-barrier energies [8,10]. For target/projectile systems with nonzero ground state spins, the projection of intrinsic spin on to the fission symmetry axis ( $K = \pm I_0$ ) makes the entrance channel  $K$ -distribution peak at  $K = \pm I_0$  [8]. This has been incorporated while calculating the angular distributions for target projectile systems with nonzero ground state spins. Figures 4 and 5 show examples of our calculations for systems with nonzero ground state spin along with the experimental data for the same values of  $x$  and  $q$ . It is seen that the calculations are in very good agreement with the data. From the best fit value of  $q$  given

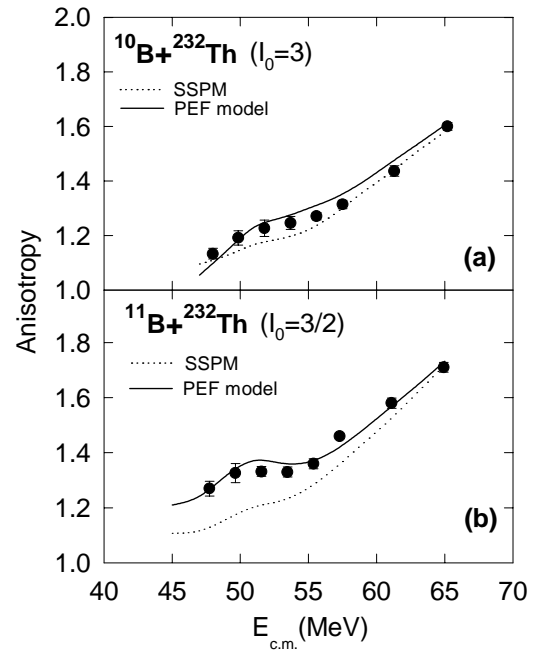


FIG. 4. Same as Fig. 2 for  $^{10}\text{B}+^{232}\text{Th}$  and  $^{11}\text{B}+^{232}\text{Th}$  systems [10] corresponding to ( $\alpha > \alpha_{BG}$ ) and projectiles with nonzero spins.

above, and taking a temperature of 1 MeV, we infer a  $K$  equilibration time of  $\sim 6 \times 10^{-20}$  s. The best fit value of  $x \approx 0.3$  suggests that the NCNF events can arise due to the PEF mechanism when quasifission is not expected. Hinde *et al.* [7] had proposed that in case of deformed target nuclei, quasifission may still take place due to collisions with the tips of prolate deformed nuclei, and they tried to explain, on this basis, the anomalous fragment anisotropies in  $^{16}\text{O}$  induced fission of  $^{238}\text{U}$  observed close to the fusion barrier.

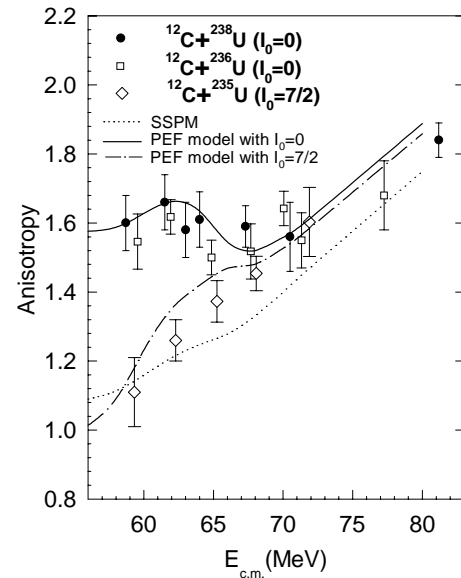


FIG. 5. PEF model predictions for systems with nonzero target ground state spins. The calculations (solid line) for the spin-zero  $^{12}\text{C}+^{238}\text{U}$  system is also shown for comparison. Experimental data taken from Ref. [8].

When quasifission is important, nucleon emission leading to evaporation residues should be suppressed. But recent results of Sonzogni *et al.* [17] on excitation function for the  $4n$  evaporation residues from the  $^{12}\text{C} + ^{236}\text{U}$  reaction at energies between 62 and 73 MeV do not show any appreciable quasifission competition. In another recent study of  $^{12}\text{C}$ ,  $^{19}\text{F}$ , and  $^{30}\text{Si}$  induced reactions of  $^{204}\text{Pb}$ ,  $^{197}\text{Au}$ , and  $^{186}\text{W}$ , Berriman *et al.* [18] have reported that the compound-nucleus formation is suppressed for the case of heavier projectiles even though theoretically one does not expect quasifission contributions for such low values of  $Z_1 Z_2$ . The observed suppression of compound-nucleus formation by Berriman *et al.* again points to the presence of preequilibrium fission in these reactions.

In conclusion, it is shown that the mechanism of preequilibrium fission, which is conceptually different from quasifission and fast fission, contributes to non-compound-nucleus fission for  $\alpha < \alpha_{BG}$  systems at all energies and even for  $\alpha > \alpha_{BG}$  at sub-barrier energies. The fission fragment angular distributions calculated as an admixture of compound nuclear and preequilibrium components are able to explain consistently the energy dependence of the angular anisotropies at energies both well below and above the Coulomb barrier for many systems involving the actinide targets. Thus the fragment anisotropies serve as a probe of the fusion-fission dynamics and can be used as a guide in selecting optimum entrance channel conditions for the synthesis of superheavy nuclei.

- 
- [1] V.S. Ramamurthy *et al.*, Phys. Rev. Lett. **65**, 25 (1990).  
 [2] S. Kailas, Phys. Rep. **284**, 381 (1997).  
 [3] B.B. Back *et al.*, Phys. Rev. C **32**, 195 (1985).  
 [4] V.S. Ramamurthy and S.S. Kapoor, Phys. Rev. Lett. **54**, 178 (1985).  
 [5] S. S. Kapoor, *Nuclear Fission Research with Medium Energy Heavy Ion Beams* (Indian Science Congress, 1994).  
 [6] D. Vorkapic and B. Ivanisevic, Phys. Rev. C **52**, 1980 (1995).  
 [7] D.J. Hinde *et al.*, Phys. Rev. Lett. **74**, 1295 (1995).  
 [8] J.P. Lestone, A.A. Sonzogni, M.P. Kelley, and R. Vandenbosch, Phys. Rev. C **56**, R2907 (1997).  
 [9] J.C. Mein *et al.*, Phys. Rev. C **55**, R995 (1997).  
 [10] B.K. Nayak *et al.*, Phys. Rev. C **62**, 031601(R) (2000).  
 [11] Yu.Ts. Oganessian *et al.*, Nature (London) **400**, 242 (1999).  
 [12] Yu.Ts. Oganessian *et al.*, Phys. Rev. C **63**, 011301(R) (2001).  
 [13] W.J. Swiatecki, Phys. Scr. **24**, 113 (1981).  
 [14] V.S. Ramamurthy, A.K. Mohanty, S.K. Kataria, and G. Rangarajan, Phys. Rev. C **41**, 2702 (1990).  
 [15] T. Dossing and J. Randrup, Nucl. Phys. **A433**, 215 (1985).  
 [16] A.J. Sierk, Phys. Rev. C **33**, 2039 (1986).  
 [17] A.A. Sonzogni, R. Vandenbosch, A.L. Caraley, and J.P. Lestone, Phys. Rev. C **58**, R1873 (1998).  
 [18] A.C. Berriman, D.J. Hinde, M. Dasgupta, C.R. Morton, R.D. Butt, and J.O. Newton, Nature (London) **413**, 144 (2001).  
 [19] Zuhua Liu *et al.*, Phys. Rev. C **54**, 761 (1995).  
 [20] R. Vandenbosch *et al.*, Phys. Rev. C **54**, R977 (1996).  
 [21] D.J. Hinde *et al.*, Phys. Rev. C **53**, 1290 (1996).